Australasian Physical & Engineering Sciences in Medicine (2019) 42:995–1009
https://doi.org/10.1007/s13246-019-00798-7

SCIENTIFIC PAPER

Feasibility of novel in vivo EPID dosimetry system for linear accelerator quality control tests

Fatih Biltekin[1] · Yagiz Yedekci[1] · Gokhan Ozyigit[1]

Received: 9 May 2019 / Accepted: 4 September 2019 / Published online: 12 September 2019

Abstract

The main aim was to validate the capability of a novel EPID-based in vivo dosimetry system for machine-specific quality control (QC) tests. In current study, two sets of measurements were performed in Elekta Versa HD linear accelerator using novel iViewDose™ in vivo dosimetry software. In the first part, measurements were carried out to evaluate the feasibility of novel in vivo system for daily dosimetric QC tests including output constancy, percentage depth dose (PDD) and beam profile measurements. In addition to daily QC tests, measured output factor as a function of field size, leaf transmission and tongue and groove effect were compared with calculated TPS data. In the second part of the measurements, detection capability of iViewDose software for basic mechanical QC tests were investigated for different setup conditions. In dosimetric QC tests, measured output factor with changing field size, PDD, beam profile and leaf transmission factors were found to be compatible with calculated TPS data. Additionally, the EPID-based system was capable to detect given dose calibration errors of 1% with ± 0.02% deviation. In mechanical QC tests, it was found that iViewDose software was sensitive for catching errors in collimator rotation (≥ 1°), changes in phantom thickness (≥ 1 cm) and major differences in irradiated field size down to 1 mm. In conclusion, iViewDose was proved to be as useful EPID-based software for daily monitoring of linear accelerator beam parameters and it provides extra safety net to prevent machine based radiation incidents.

Keywords Quality control · EPID · Linear accelerator

Abbreviations

2D	Two-dimensional
3D	Three-dimensional
DRP	Dose reference point
BEV	Beam's eye view
CT	Computed tomography
DD	Dose differences
DICOM	Digital imaging and communications in medicine
DTA	Distance to agreement
EPID	Electronic portal imaging device
IMRT	Intensity modulated radiotherapy
MLC	Multileaf collimator
MU	Monitor unit
PDD	Percentage depth dose
RT	Radiotherapy
SBRT	Stereotactic body radiation therapy
SRS/SRT	Stereotactic radiosurgery/radiotherapy
SSD	Source to surface distance
TPS	Treatment planning system
QC	Quality control
VMAT	Volumetric modulated arc therapy

Introduction

Electronic portal imaging device (EPID) was initially developed as an imaging tool to localize target volume and to verify patient position. However, it was later realized that image pixel or signal obtained with EPID system was also related with delivered dose to the patient [1]. Not long after its introduction for dose verification, dosimetric properties of the EPID were studied by several groups [2, 3] and it has proven to be reliable and accurate dose verification method to validate the feasibility of complex treatment techniques like intensity modulated radiotherapy (IMRT), volumetric modulated arc therapy (VMAT) and stereotactic radiosurgery/radiotherapy (SRS/SRT) [4]. In addition to pre-treatment dose verification, EPID was currently defined as one of the most promising in vivo dosimetry system

✉ Fatih Biltekin
fatih.biltekin@hacettepe.edu.tr

[1] Department of Radiation Oncology, Faculty of Medicine, Hacettepe University, 06100 Ankara, Turkey

providing two dimensional (2D) and three dimensional (3D) information of delivered dose to the patient during the treatment [5, 6]. Despite the obvious advantages of portal dosimetry in patient-specific quality control (QC) and in vivo dose measurements, the use of EPID is still limited worldwide. However, several groups [4, 7–10] have already developed their own software to use EPID as an in vivo dosimetry and they reported long-term results of in vivo dose measurements. Additionally, manufacturers have recently offered some sophisticated solutions for EPID-based in vivo dose measurements to overcome this problem. One of the introduced solutions is iViewDose™ software (Elekta AB, Stockholm, Sweden) developed with the collaboration of Elekta AB and The Netherlands Cancer Institute—Antoni van Leeuwenhoek Hospital. This software provides an end-to-end verification of the real treatment by taking an on line MV image during irradiation [9, 11]. iViewDose uses a sophisticated back-projection algorithm to convert EPID signal to absorbed dose in 3D reconstructed patient plane and it is capable to detect major errors including systematic and random machine errors, treatment planning and dose calculation errors, anatomical changes, setup deviations and data transfer errors. All defined features of the software make it as a promising solution to minimize the radiation incidents or errors during radiotherapy (RT) facilities. However, the back-projection algorithm used in the iViewDose software uses a water-based scatter-correction kernels and the accuracy of dose reconstruction model is not adequate in the presence of large inhomogeneities such as lung. Therefore, in heterogeneous medium *in aqua vivo* method is suggested to minimize the dose reconstruction errors during calculation. The basic idea behind *in aqua vivo* dosimetry is based on to convert EPID images taken in inhomogeneous medium to a situation as if the patient consisted entirely of water. For dose verification, reconstructed dose distribution in homogenous medium needs to be compared with reference treatment plan calculated with the tissue inhomogeneity correction switched off [12]. Although, iViewDose software was primarily introduced for in vivo dose measurements and patient-specific QC during actual treatment, in the present study it was aimed to validate this novel system for machine-specific QC tests to alleviate the workload of daily measurements. To the best of our knowledge, this is the first study to evaluate the feasibility of Elekta iViewDose software in machine-specific QC tests using 3D dose analysis.

Materials and methods

Equipment and image acquisition

All measurements were carried out on Elekta Versa HD linear accelerator (Elekta AB, Stockholm, Sweden) equipped with Agility collimator consisting of 80 leaf pairs with a projected leaf width 0.5 cm at the beam isocenter and EPID iViewGT v.3.4.1 MV panel (Elekta AB, Stockholm, Sweden). The EPID is mounted at a source to surface distance (SSD) of 160 cm and has a sensitive area of 41 × 41 cm corresponding to a field size of 26 × 26 cm at the beam isocenter. EPID-based iViewDose v.1.0.1 software works in conjunction with the existing MV panel and iViewGT image acquisition system. After image acquisition process, iViewDose software convert detected signal to the absolute dose value in the reconstruction plane estimated from computed tomography (CT) data of the phantom or patients. Then, reconstructed dose distribution can be compared with calculated dose distribution using 3D γ analysis method.

In the present study, two sets of measurements including dosimetric and mechanical QC tests were performed to validate the feasibility of novel in vivo dosimetry for machine-specific QC tests. To perform these QC tests, CT of the RW3 solid water phantom (PTW, Freiburg, Germany) with dimensions of 30 cm × 30 cm × 20 cm in x, y and z directions were scanned using 100 kVp tube voltage, 300 mAs tube current and 2.5 mm slice thickness. As a treatment planning system (TPS) RayStation v. 7.1.0 (RaySearch Lab., Stockholm, Sweden) was used and calculation grid size was selected as $0.3 \times 0.3 \times 0.3$ cm^3 for dose calculation.

Dosimetric QC tests

Dosimetric QC tests were performed in six steps as summarized in Table 1. In the first step, output factor corrections as a function of photon beam field size were measured with EPID and analyzed with iViewDose software. The results were then compared with beam data measurements obtained with microDiamond type 60,019 (PTW, Freiburg, Germany) detector and calculated TPS data. As a definition, output factor was calculated as the ratio of the dose in a given field size (2 × 2, 5 × 5, 10 × 10, 15 × 15 and 20 × 20 cm) to the dose of a reference field size (10 × 10 cm) at the depths of 10 cm with a nominal SSD of 100 cm. In the second step, EPID-based in vivo dosimetry system was applied to check the percentage depth dose (PDD) and beam profile for open field sizes as given in Table 1. Additionally, to evaluate the performance of iViewDose software for complex static fields, Z-letter and finger pattern MLC shapes were created in the TPS. In the finger pattern MLC shapes, treatment plan consisted of two static fields with overlapping MLC positions having a 0.5 cm width between two MLC edges as shown in Fig. 1. The open region in the first static field was covered by the MLC protrusion in the second field, totally covering a field area of 15 × 15 cm and both of these treatment fields were irradiated consecutively and measured line profile was compared with TPS data. In the third step, beam profiles were measured for different wedge angles and measured data with EPID system was compared with in-plane beam profile calculated in TPS. In the third-fourth step of

Table 1 The methodology for dosimetric QC tests

Dosimetric QC tests	
Linac	Elekta Versa HD
3D γ evaluation criteria	3 mm DTA/3% DD
	ΔDRP ≤ 3%, γ mean ≤ 0.5, γ 1% ≤ 3 and
	% γ ≤ 1 greater than or equal to %85
Energy	6 MV and 6 FFF for Part I, II, IV, V, VI11 (VI)
	6 MV for Part III
SSD (cm)	100
Part I: output factors	
Field size (cm)	2 × 2, 5 × 5, 10 × 10, 15 × 15 and 20 × 20
DRP depth (cm)	10
Part II: PDD and profile	
Field size: open field size (cm)	Profile: 2 × 2, 5 × 5, 10 × 10, 15 × 15 and 20 × 20
	PDD: 10 × 10
Field shape: irregular field	Modified finger pattern and Z-letter
Depth (cm)	Beam profile: at 10 cm for open and irregular fields
	PDD: from surface to 20 cm depth
Part III: profile (wedged field)	
Motorized wedge angle (°)	15, 30, 45 and 60
Field size (cm)	10 × 10
Depth (cm)	10
Part IV: transmission (intra- and inter leaf)	
Field size: MLC shaped	2 × 2
Measured DRP distance (cm)	For interleaf: 3 cm from the edge of 2 × 2 cm MLC shaped field
	For intraleaf: 3.25 cm from the edge of 2 × 2 cm MLC shaped field
DRP depth (cm)	1.5
Part V: dose calibration errors	
Field size (cm)	10 × 10
DRP depth (cm)	1.5
Errors (%)	1, 2, 5
Part VI: dose rate and linearity	
Field size (cm)	10 × 10
DRP depth (cm)	1.5
Monitor unit (MU)	1, 2, 5, 10, 25, 50, 100, 200, 500 and 1000 for linearity
Dose rate (MU/dk)	70, 250, 500 for 6 MV and 70, 150, 340, 680, 1000, 1400 for 6 FFF

the measurement, calculated and measured MLC transmission factors were analyzed to evaluate the capability of novel in vivo dosimetry system in leaf transmission measurements. Additionally, inter- and intra-leaf transmission was measured with microDiomand detector. In another step, feasibility of iViewDose system was analyzed to decrease the workload of ionization chamber-based measurement in daily output check. To evaluate the detection sensitivity of the system 1%, 2% and 5% dose calibration errors were created for 6 MV and 6 FFF photon energies in the treatment machine. All dose calibration errors were validated with 0.6 cc Farmer-type ionization chamber (PTW, Freiburg, Germany) and results were analyzed with iViewDose software. In the last part of the dosimetric QC tests, dose rate dependence and linearity of the EPID system were investigated for defined conditions in Table 1.

Mechanical QC tests

As given in Table 2, the feasibility of novel EPID-based in vivo dosimetry system for basic mechanical QC tests was evaluated in four steps. In the first step, two different scenarios were created for the symmetric field size of 10 × 10 cm to evaluate the sensitivity of EPID system for catching errors in radiation field size. In the first scenario, 1 mm and 2.5 mm errors were given in the same direction (e.g. Y1: 4.9 cm, Y2: 5.1 cm for 1 mm error in each axis and Y1: 4.75 cm, Y2: 5.25 cm for 2.5 mm error in each axis) and opposite

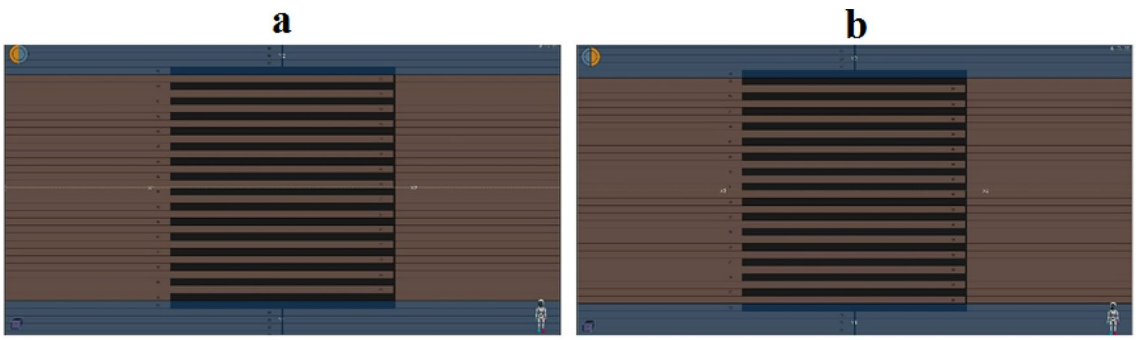

Fig. 1 Beam's eye view (BEV) of the finger pattern MLC shaped fields; **a** first field and **b** second field

Table 2 The methodology for mechanical QC tests

Mechanical QC tests	
Linac	Elekta versa HD
3D γ evaluation criteria	3 mm DTA/3% DD
	ΔDRP ≤ 3%, γ mean ≤ 0.5, γ 1% ≤ 3 and
	% γ ≤ 1 greater than or equal to %85
Energy	6 MV
Part I: light and radiation field size coincidence	
Field size: symmetric (cm)	10 × 10
Field size: asymmetric (cm)	1: X1: − 5, X2: 0, Y1: − 5 and Y2: 0
	2: X1: − 5, X2: 0, Y1: 0 and Y2: + 5
	3: X1: 0, X2: + 5, Y1: 0 and Y2: + 5
	4: X1: 0, X2: + 5, Y1: 0 and Y2: − 5
Errors (mm)	Symmetric: (i) ± 1 and ± 2.5 mm errors in the same and opposite directions for Y1 and Y2 jaws (ii) ± 2 mm and ± 5 mm errors for only Y1 directions
	Asymmetric: ± 2 mm and ± 5 mm total errors for Y directions in the center of the field
SSD (cm)	90 (source to axis distance at 10 cm is equal to 100 cm)
Depth (cm)	10
Part II: Gantry and Collimator	
Field Size (cm)	10 × 10
SSD (cm)	90 (source to axis distance at 10 cm is equal to 100 cm)
Depth (cm)	10 cm
Erros (°)	1, 2 and 5
Part III: SSD differences	
Field Size (cm)	10 × 10
Reference SSD (cm)	100
Depth (cm)	1.5 cm for beam profile and DRP
Errors (cm)	0.5, 1 and 2 (current SSD value: 99.5, 99 and 98 cm)
Part IV: changes in phantom thickness	
Field size (cm)	10 × 10
SSD (cm)	90 (source to axis distance at 10 cm is equal to 100 cm)
Reference depth (cm)	10
Errors (cm)	1, 2 and 5 cm pahntom thickness errors from the reference conditions (current depth value: 9, 8 and 5 cm)

direction (e.g. Y1: 5.1 cm, Y2: 5.1 cm for 1 mm error in each axis and Y1: 5.25 cm, Y2: 5.25 cm for 2.5 mm error in each axis) for Y1 and Y2 jaws. Total error was set as 2 mm and 5 mm in Y axis, respectively. In the second scenario, ± 2 mm and ± 5 mm errors (e.g. Y1: 4.8 cm, Y2: 5.0 cm for − 2 mm error and Y1: 5.5 cm, Y2: 5.0 cm for + 5 mm error in Y1 axis) were created in only Y1 directions. All treatment plans for a given errors in both scenarios were created in the TPS and transferred to the iViewDose software. Dose line profiles calculated in TPS were then matched with EPID measurements to quantify the size of errors indirectly. In addition to EPID-based measurements, EBT3 gafchromic film (Ashland Specialty Ingredients, NJ, USA) with isocentric beam checker was used to validate field size for each axis. In the second step, detection sensitivity of novel in vivo dosimetry system was evaluated for a given errors of 1°, 2° and 5° in gantry and collimator rotation in the treatment machine. All measurements were compared with the reference conditions of 0° created in TPS. In another step, measurement was performed to evaluate the capability of novel in vivo dosimetry system for catching 0.5 cm, 1 cm and 2 cm errors in SSD value. Finally, changes in phantom thicknesses were simulated by removing 1 cm, 2 cm and 5 cm phantom material from the upper part of the reference phantom geometry. All measurement were compared with the reference treatment plan calculated in TPS and sensitivity of the novel system for detecting changes in phantom thicknesses was evaluated using gamma passing rate and dose differences at d_{max}.

γ evaluation

EPID-reconstructed and calculated dose distribution were analyzed using 3D γ analysis method. As an evaluation criterion, 3 mm distance to agreement (DTA) and 3% dose differences (DD) were used. Pass-fail criteria of the treatment planning is based on the differences in dose reference point (DRP), mean γ value, the maximum 1% γ value and the percentage of points with $\gamma \leq 1$ within the 50% isodose surface of the planned maximum dose. Passing limits for the criteria were defined in Tables 1 and 2. Additionally, measured and calculated line profiles in central axis and in defined depth were analyzed for PDD and beam profile comparison, respectively. The same line profile comparison was performed to analyze the detectability of light and radiation field coincidence with given errors in symmetric and asymmetric fields.

Results

Dosimetric QC tests

Comparison of output factor corrections as a function of field size were given in Table 3. EPID-based measurements were found to be compatible with beam data and modelled TPS calculation up to 20 × 20 cm field size for 6 MV and 6 FFF photon energies. Point dose differences between EPID and TPS at 10 cm depth were smaller than 1% for all field sizes and maximum dose differences were detected as 0.86% in 2 × 2 cm field size for both photon energies. However, differences in normalized output factor corrections were lower than ± 0.4%.

As illustrated in Figs. 2, 3, beam profiles of the all fields were well matched with TPS data. According to 3D γ analysis results, % $\gamma \leq 1$ or gamma passing rate value for all field size were greater than 85% in defined phantom geometry. However, most of the failed points in 3D γ analysis were observed in the penumbra and build up region of the irradiated fields. In PDD measurement, results were also compatible with TPS data in 2.7% for 6 MV and 1.5% for 6 FFF photon energies as shown in Fig. 4. In 6 MV photon energy, maximum differences in PDD was observed in build-up region and depths over than 15 cm. The main reason can be associated with differences in commissioning data in EPID-based measurements and electron contamination unaccounted in the reconstruction model used in iViewDose software. However, all these data were in the tolerance limits of 3%. In addition to open field size, beam profile measurements for different wedge angles were performed using 6 MV photon energies as illustrated in Fig. 5. EPID-based

Table 3 Calculated and measured output factor as a function of field sizes for 6 MV and 6FFF photon energies

Field Size (cm)	6 MV TPS (beam data**)	6 MV iViewDose	Relative difference (%)	6 FFF TPS (beam data**)	6 FFF iViewDose	Relative difference (%)
2 × 2	0.779 (0.778)	0.781	0.26 (0.39)	0.840 (0.838)	0.841	0.12 (0.36)
5 × 5	0.906 (0.906)	0.907	0.11 (0.11)	0.980 (0.980)	0.981	0.1 (0.1)
10 × 10*	1.000 (1.000)	1.000	–	1.000 (1.000)	1.000	–
15 × 15	1.057 (1.056)	1.057	0 (0.09)	1.104 (1.103)	1.105	0.09 (0.18)
20 × 20	1.094 (1.093)	1.095	0.09 (0.18)	1.124 (1.243)	1.125	0.09 (0.18)

*All measured values were normalized to 10 × 10 cm

**Measurement taken with microDiamond type 60,019 detector

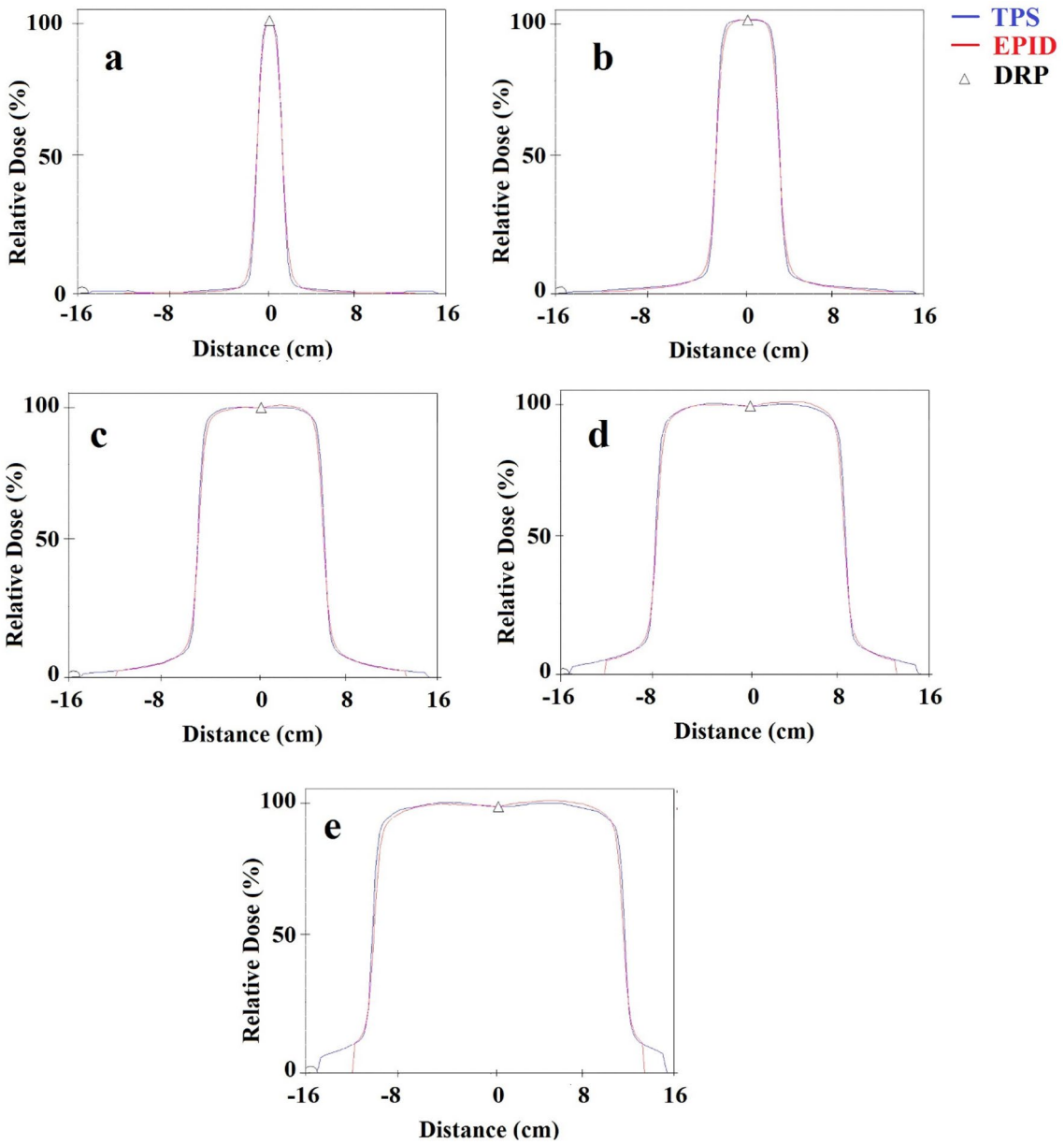

Fig. 2 Measured (red) and calculated (blue) beam profile (in-plane direction) for defined field sizes; **a** 2×2 cm, **b** 5×5 cm, **c** 10×10 cm, **d** 15×15 cm and **e**) 20×20 cm using 6 MV photon energy and Δ (DRP) indicates the central axis of the beam profile at 10 cm depth

measurements were found to be consistent with TPS data for different motorized wedge angles.

Beam profiles of Z-letter shape field at 10 cm depth were illustrated in Fig. 6c and d for 6 MV and 6 FFF photon energies, respectively. According to 3D γ evaluation, percentage of points with $\gamma \leq 1$ within the 50% isodose surface of the planned maximum dose was found as 87% and 84.5% for 6 MV and 6 FFF, respectively. When the gamma evaluation criteria was changed as 3.5% DTA and 3.5% DD, gamma passing rate were increased up to 94.5%. In the finger pattern MLC test, significant difference was observed between measured and calculated dose line profile in both measurement planes. Measured in-plane dose profile had significantly deeper wells than the calculated profile for 6 MV and 6 FFF in TPS as shown in Figs. 7, 8b, respectively. For instance in 6 MV photon energy, the depths of the measured wells were approximately 80% and 120% of the normalized central axis dose of the measured beam profile. However, calculated wells amounted approximately 95% and 105% of the normalized central axis dose. These differences indicated inadequate modeling of the tongue and groove effect in TPS. Additionally, significant difference was detected between measured and calculated dose profile in cross-plane directions (Figs. 7c and 8c). Although,

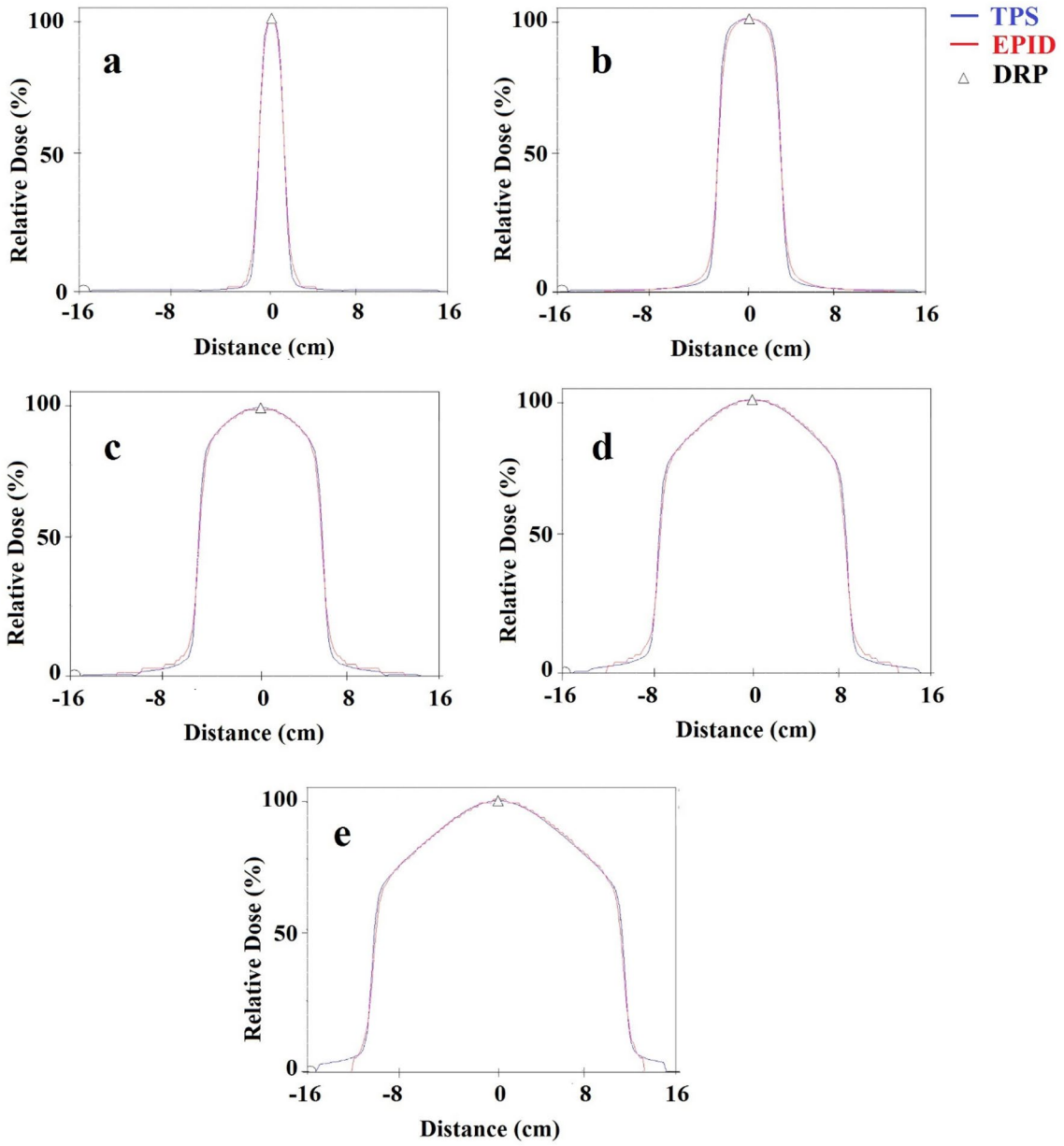

Fig. 3 Measured (red) and calculated (blue) beam profile (in-plane direction) for defined field sizes; **a** 2×2 cm, **b** 5×5 cm, **c** 10×10 cm, **d** 15×15 cm and **e** 20×20 cm using 6 FFF photon energy and Δ (DRP) indicates the central axis of the beam profile at 10 cm depth

calculated minimum static leaf gap between opposing leaves was in principle 0.1 cm at the MLC itself to maintain a separation of 0.5 cm at the isocentric plane, measured minimum static leaf gap was found as almost four fold of the accounted gap in the TPS. According to our measurements, calculated dose distribution in TPS underestimates the effects of static leaf gap at the edge of the static treatment field closed with MLC. Therefore, this gap should be taken into consideration in MLC shaped complex static fields, especially for field-in-field techniques used in forward IMRT. Our measurement also revealed that adequate modeling of the MLC parameters like tongue and groove effect and static leaf gap by TPS is essential for accurate dose calculation especially in treatments plans using complex treatment fields and small MLC gaps.

Novel in vivo dosimetry system was also capable to measure MLC transmission. In RayStation TPS, the average of the inter- and intra-leaf transmission factor was used to model the MLC transmission. According to our measurements, inter- and intra-leaf transmissions were found as 0.51%, 0.47% for 6 MV and 0.44%, 0.41% for 6 FFF photon energies, respectively. The mean of the measured

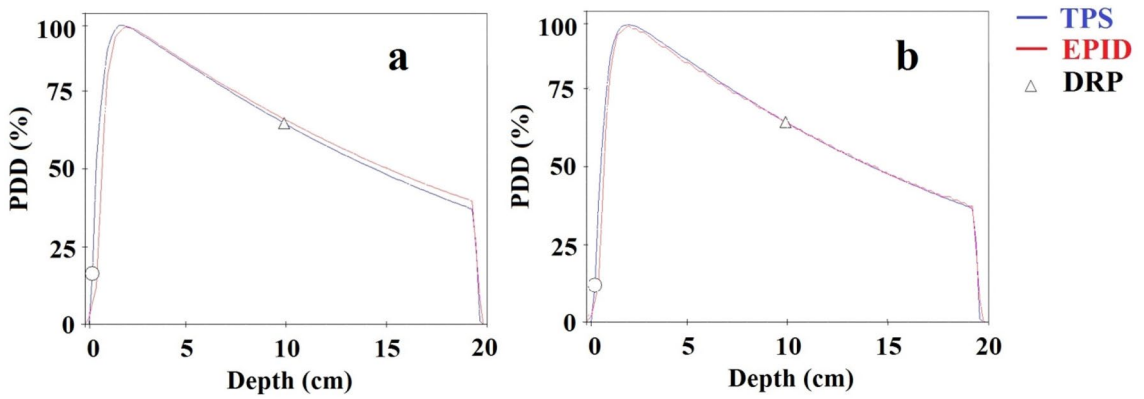

Fig. 4 Measured (red) and calculated (blue) PDD graphics for 10×10 cm field size using **a** 6 MV and **b** 6 FFF photon energies and Δ (DRP) indicates the reference point at 10 cm depth

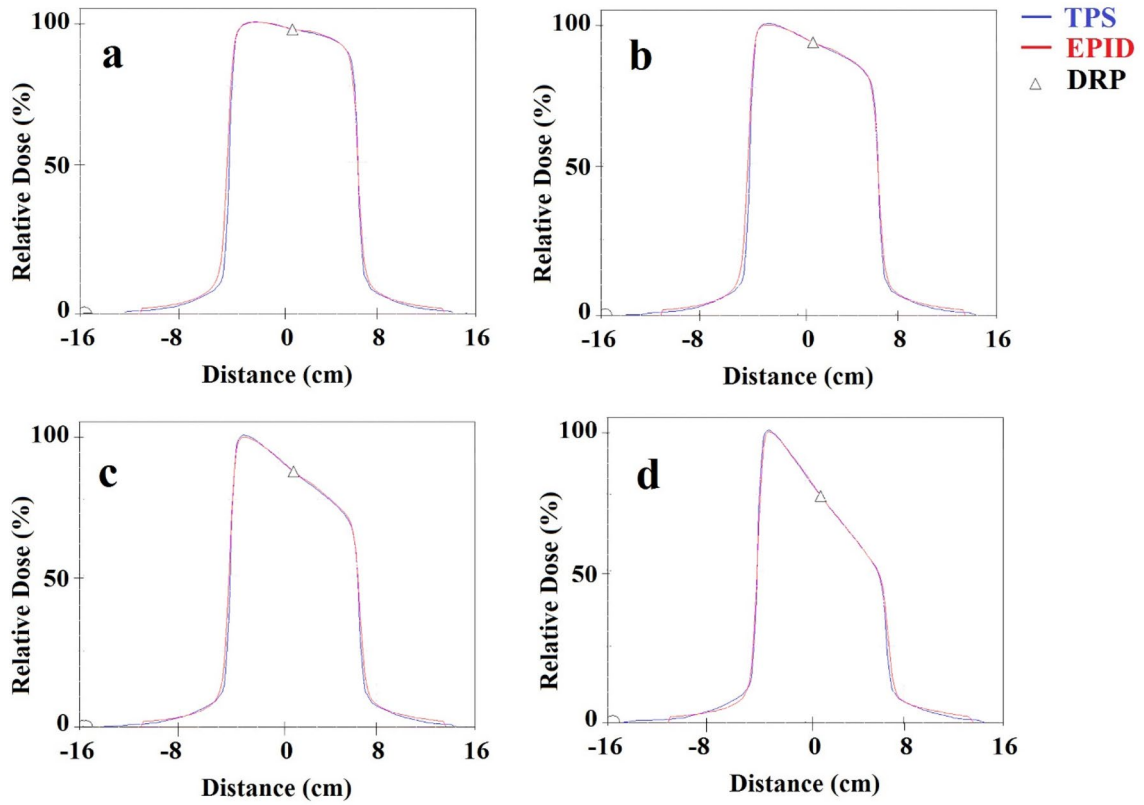

Fig. 5 Measured (red) and calculated (blue) wedged field profiles (in-plane direction); **a** 15°, b 30°, **c** 45° and **d** 60° for 10×10 cm field size using 6 MV photon energy and Δ (DRP) indicates the central axis of the beam profile at 10 cm depth

transmission factor was found to be consistent with 0.5% used in TPS for both energies. Similarly, inter- and intra-leaf transmissions measured with microDiomand were obtained as 0.64%, 0.57% for 6 MV and 0.50%0.44% for 6 FFF, respectively.

Detection sensitivity of the EPID-based in vivo dosimetry for daily dose calibration errors was found to be compatible with reference measurements. According to our measurement, 1%, 2% and 5% dose calibration errors validated with 0.6 cc Farmer-type ionization chamber were detected as 1.02%, 2.03%, 5.07% for 6 MV and 0.99%, 1.98% and 4.98% for 6 FFF photon energies, respectively.

In the last part of the measurements, maximum differences for varying dose rates was found as 0.1% at 6 MV and

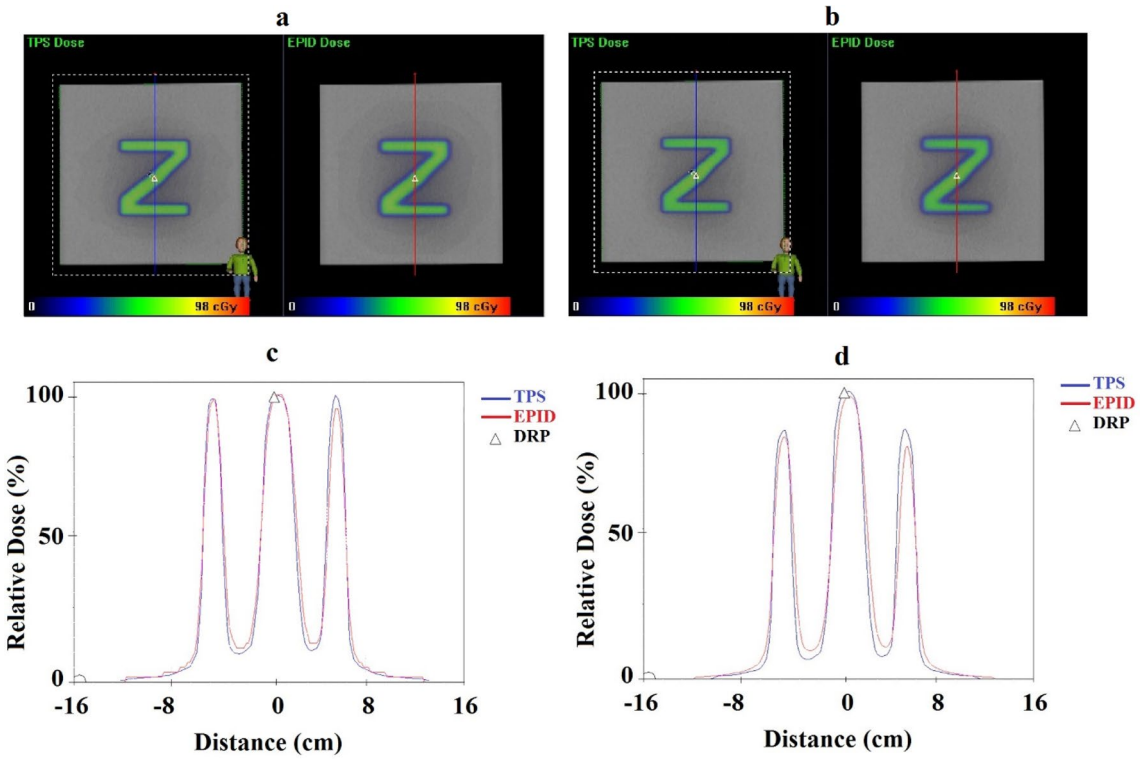

Fig. 6 Demonstration of a planned (right) and EPID reconstructed (left) dose distribution for **a** 6 MV, **b** 6 FFF and comparison of planned and EPID reconstructed in plane dose line profile for **c** 6 MV, **d** 6 FFF photon energies and Δ (DRP) indicates the central axis of the beam profile at 10 cm depth

0.4% at 6 FFF photon energies. Additionally, dose response of the EPID was linear between 1 and 1000 monitor units (MU) for defined reference conditions.

Mechanical QC Tests

According to our analysis, 1 mm and 2.5 mm field size errors in the same directions were not detected due to the automatic alignment of the treatment field. Additionally, the effect of − 1 mm errors in opposite directions was not detected in both 3D gamma evaluation and dose line profile. The reason can be attributed to existing errors in the linear accelerator, which is almost + 0.5 mm in Y1 and Y2 axis, measured with gafchromic film. Therefore, given errors in Y1 and Y2 axis were almost equal to − 0.5 mm with respect to measured field size when the sum of the total errors was calculated. However, + 1 mm and ± 2.5 mm deviation in opposite directions were detected with iViewDose in vivo dosimetry system. In this case, total errors in Y1 and Y2 axis were almost equal to + 1.5 mm, + 3 mm and − 2 mm for a given errors of + 1 mm, + 2.5 mm and − 2.5 mm in TPS, respectively. Therefore, the magnitude of the errors detected with iViewDose was found higher for + 1 mm, + 2.5 mm and lower for − 2.5 mm than errors calculated in TPS. Additionally, ± 2 mm and ± 5 mm errors in Y1 directions were detected in iViewDose software as shown in Fig. 9. In the analysis of asymmetric field coincidence, the errors in the same directions were not also detected with iViewDose software. However, even total 2 mm errors in opposite direction can be visualized in both dose distribution and dose line profile as shown in Fig. 10 and Fig. 11, respectively.

Novel EPID-based in vivo dosimetry system was also capable to detect major collimator rotation differences. According to γ analysis results, 1° and 2° collimator rotation errors caused a minimal difference in gamma analysis, but 5° rotation error led to 7% differences in gamma passing rate. Nevertheless, it was possible to measure 1° and 2° collimator rotation errors with protractor using the MV image of the irradiated field saved in iViewDose system. However, in defined setup conditions, 1°, 2° and 5° gantry angle differences were not detected in 3D γ evaluation.

Finally, SSD errors up to 2 cm were not detected with iViewDose software. However, 1, 2 and 5 cm changes in phantom thickness led to 3%, 9% and 44% differences in gamma passing rate with respect to the reference plan, respectively. Additionally, dose differences at d_{max} was increased as 1.3%, 2.7% and 6.5% for a changing phantom thickness of 1, 2 and 5 cm, respectively.

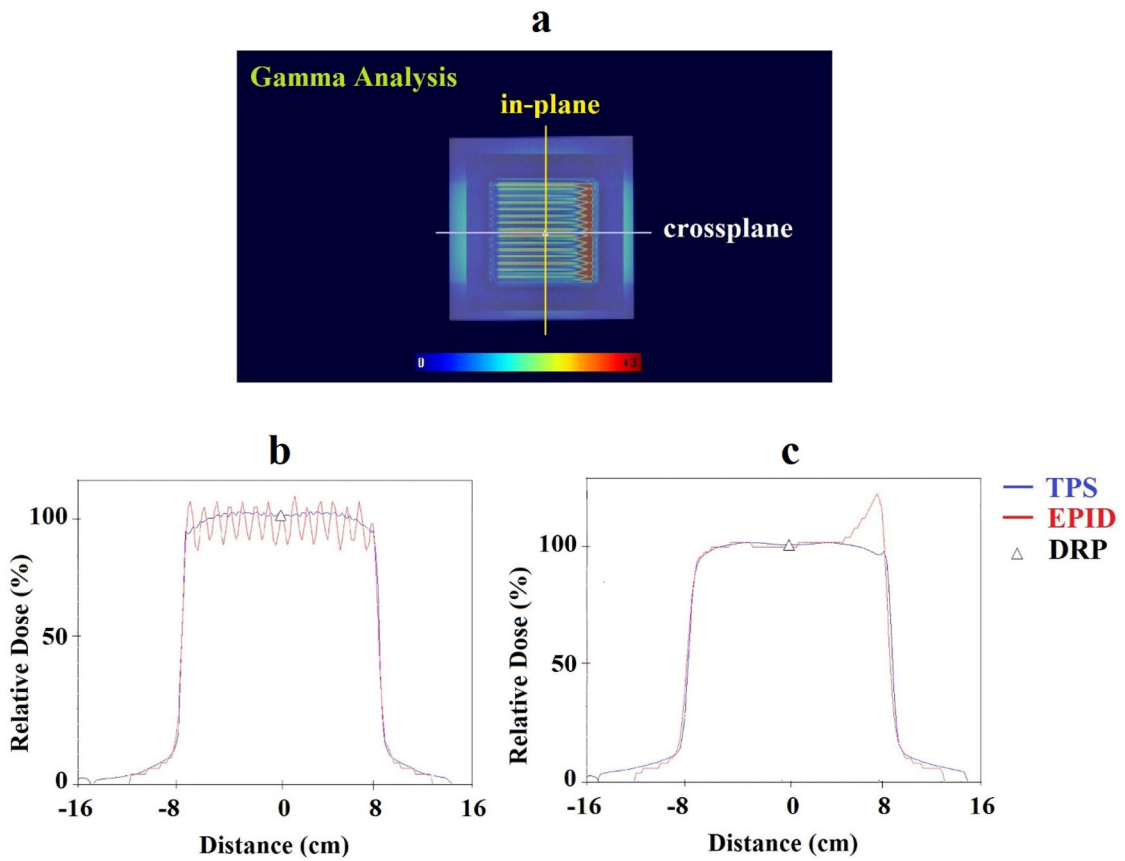

Fig. 7 Analysis of the **a** gamma distribution and dose line profiles in **b** in-plane and **c** crossplane directions for finger pattern MLC shaped field using 6 MV photon energy and Δ (DRP) indicates the central axis of the beam profile at 10 cm depth

Discussion

We have demonstrated that novel in vivo dosimetry system is capable to perform basic machine-specific QC tests including daily dose calibration, PDD and beam profile, coincidence of light and radiation field size in a single irradiation of the reference treatment field during the morning checkout of the treatment machine. Additionally, it is possible to analyze measured and calculated dose distribution as 3D for all slices and planes of the CT image. In the literature, dosimetric properties of EPID system for patient-specific QC have been studied comprehensively. However, there are limited data about the capability of EPID system for machine-specific QC test. For instance, Agarwal et al. [13] investigated the feasibility of aSi 500 II EPID system for output factor corrections and beam profile measurements of small fields from 0.8 × 0.8 cm to 10 × 10 cm using 6 and 15 MV photon energies. In the study, EPID output factors were compared with Exradin A16 microionization chamber and profiles were compared with SRS diode detector measurements. Output factors measured with EPID were in agreement (≤ 1%) with the reference data for field sizes down to 2 × 2 cm. The differences were increased up to 2.06% and 1.56% in 2 × 2 cm field size for 6 and 15 MV, respectively. Esposito et al. [6] also reported that EPID measurements were found to be compatible with microDiomand detector measurements within 2% from 2 × 2 cm to 20 × 20 cm field size in 6 MV photon energy and maximum deviation was found as 1.7% for 3 × 3 cm field size. In the present study, EPID measurements for output factor corrections were found consistent with calculated data in TPS and beam data obtained with microDiamond detector. However, in our study, maximum differences in 2 × 2 cm fields were found smaller than ± 0.4% for 6 MV. The differences can be associated with the sensitivity or image quality of EPID panel and the accuracy of the algorithm used for dose reconstruction. Similarly, in dose profile measurements our findings were found to be compatible with the measured profile by Agarwal et al. [13]. Additionally, in the literature, Sun et al. [14] and Budgell et al. [15] investigated the feasibility of EPID for daily QC of linear accelerator. Sun et al. [14] proposed a new EPID-based QC tools to monitor the daily performance of linear accelerator for defined beam parameters including output constancy, beam energy, MLC position, flatness and symmetry. They reported that measured output constancy with EPID was shown to be within ± 0.5%. Moreover, deviation

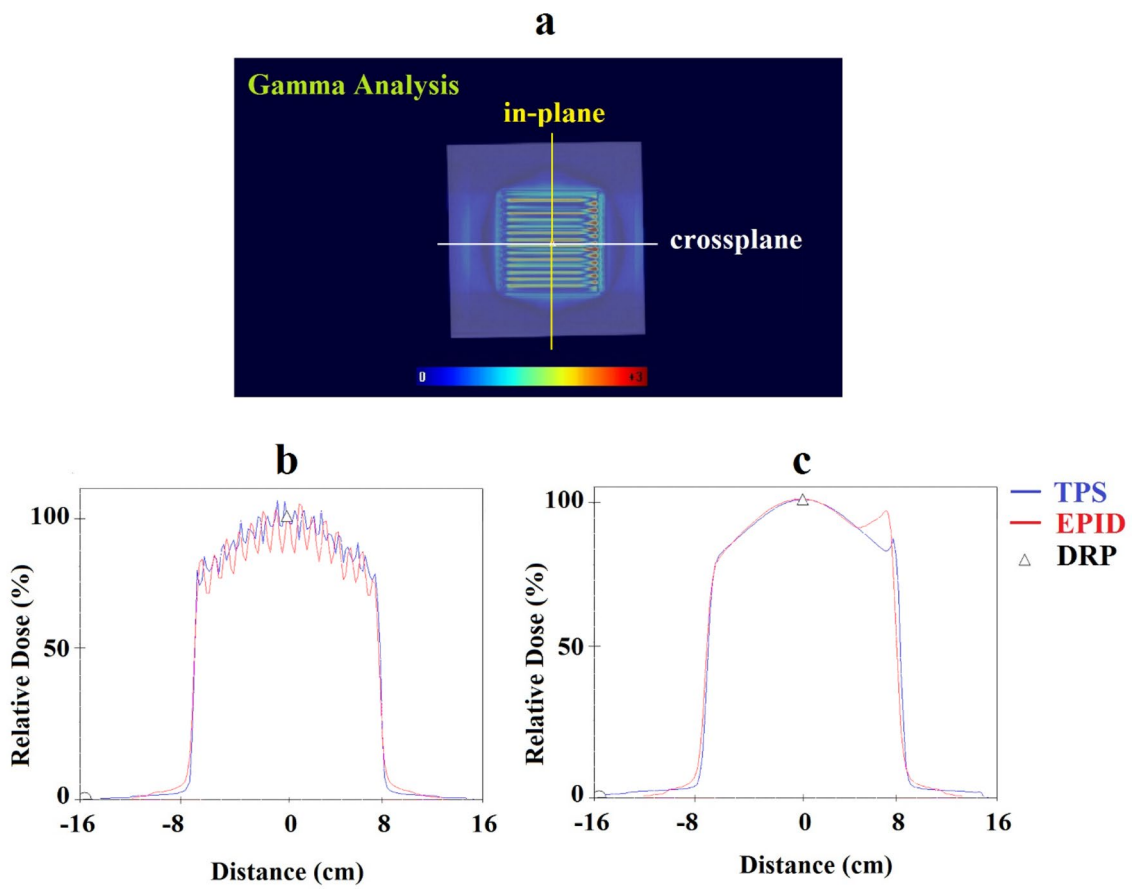

Fig. 8 Analysis of the **a** gamma distribution and dose line profiles in **b** in-plane and **c** crossplane directions for finger pattern MLC shaped field using 6 FFF photon energy and Δ (DRP) indicates the central axis of the beam profile at 10 cm depth

in flatness and symmetry were found to agree within ± 0.5% and ± 1.2% for cross-line and in-line profiles, respectively. Similarly, in the study performed by Budgell et al. [15] EPID was proved to be as useful device for daily monitoring of linear accelerator beam parameters such as output constancy, field size detection, flatness and symmetry. In the present study, output deviation was detected within ± 0.1% sensitivity for given errors of 1%, 2% and 5% which is agreed with the results reported by Sun et al. [14]. Moreover, as illustrated in Figs. 2 and 3, measured beam profile with EPID system were also well matched with calculated line profile in TPS.

In the literature, there are limited studies about the use of EPID detector for beam energy detection and PDD measurement. Dawoud et al. [16] presented a method for measuring photon beam energy with EPID. This method was based on fitting a second order polynomial to the profiles of physically wedged beams and the used metric of interest was the second order coefficient α. Then, the relationship between α and reference PDD value measured with semiflex ionization chamber at 10 cm was examined to produce a calibration curve. In the study, EPID image analysis of physically wedged beam profiles was found as a useful technique to measure linear accelerator photon beam energy, but this technique was not suitable for the PDD measurement. In contrast to Dawoud et al. [16], van Elmpt et al. [17] developed a Monte Carlo based method to reconstruct the delivered dose. They reported that reconstructed PDD values were in good agreement with reference data. However, they observed small differences in the build-up region. In the present study, PDD values reconstructed with iViewDose system were also found to be compatible with beam data measurements and similar differences were observed in the build-up region. As van Elmpt et al. [17] stated, this could be related with the electron contamination unaccounted in the reconstructed model.

Another noteworthy point is that EPID detector used in the present study was found as sensitive for detecting tongue and groove effect. According to our measurement, the tongue and groove effect had obviously larger contribution than accounted by RayStation TPS. Hægeland [18] also reported the same differences for 6 MV photon energies using gafchromic film. Therefore, this effect should be taken into consideration in complex shaped fields.

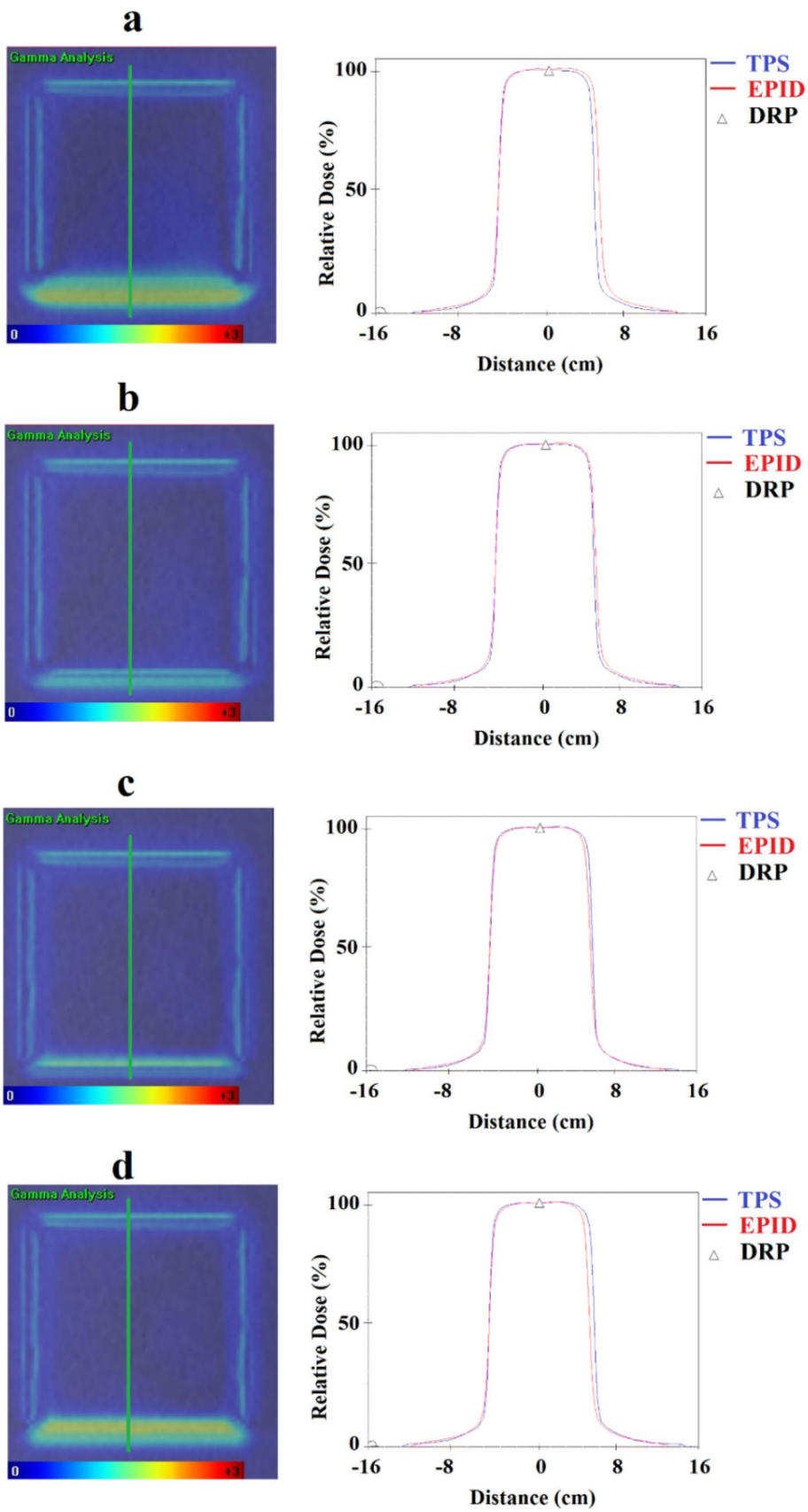

Fig. 9 Detection of the field size errors using gamma distribution (in the left side) and dose line profile (in the right side) of the reference field; **a** − 5 mm, **b** − 2 mm, **c** 2 mm and **d** 5 mm errors in Y1 directions and Δ (DRP) indicates the central axis of the beam profile at 10 cm depth

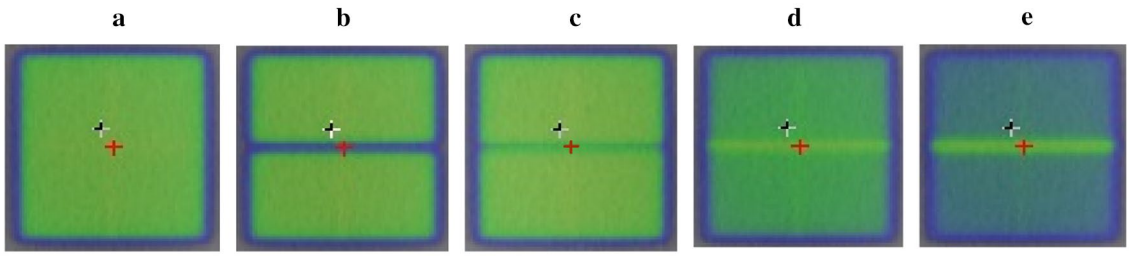

Fig. 10 Dose distribution of irradiated asymmetric fields for a given total errors of; **a** 0 mm (reference field), **b** − 5 mm, **c** − 2 mm, **d** 2 mm and **e** 5 mm in the opposite directions of Y1 and Y2 jaws

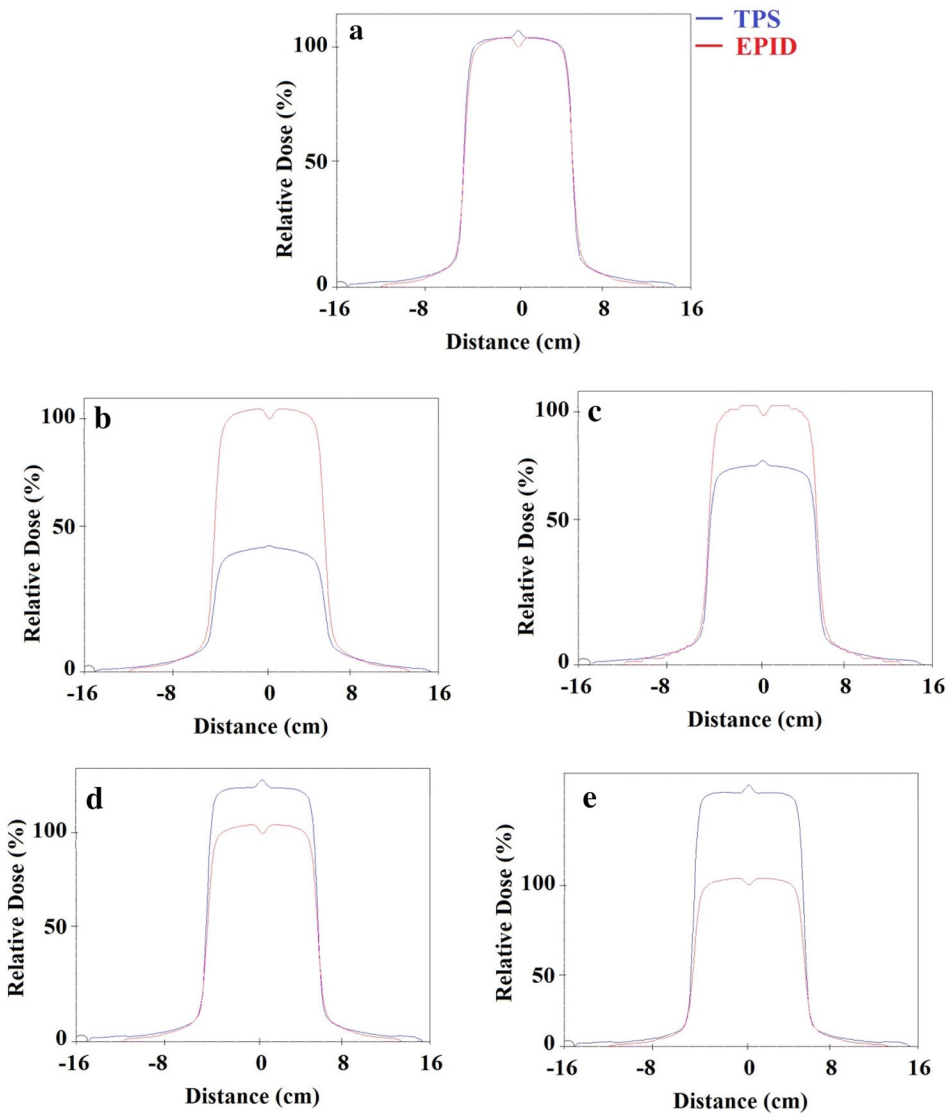

Fig. 11 Crossplane dose profile of the irradiated asymmetric fields for a given total errors of; **a** 0 mm (reference field), **b** − 5 mm, **c** − 2 mm, **d** 2 mm and **e** 5 mm in the opposite directions of Y1 and Y2 jaws

In addition to dosimetric QC test, iViewDose system was also found to be capable for detecting field size errors down to 1 mm in one or opposite directions. However, errors in the same directions were not detected by the software due to the auto alignment of the irradiated field. It can be illustrated as an important defect of the system, which should be improved by the vendor. Novel system had also capability for catching major errors (≥ 1°) in collimator rotation and

changes in phantom thickness down to 1 cm. Similarly, in the study performed by Esposito et al. [6], collimator rotation errors and anatomical variations were simulated for 4 VMAT plans in different anatomical sites (prostate, whole pelvis, head and neck, lung) to evaluate the detection sensitivity of Dosimetry Check™ (Math Resolution, LCC) (DC) software working in conjunction with the existing MV EPID Panel. They reported that EPID was sensitive to detect 1° and 2° collimator rotation errors in all plans but whole pelvis and DC software was proved to be able to detect anatomical changes which are simulated by adding 1 cm bolus to the upper part of the phantom and by removing 2 cm phantom from the central part of the reference phantom geometry.

Our EPID-based approach is a fast and accurate method to monitor daily performance of the linear accelerator and it is less time consuming than other existing methods like ionization chamber for daily dose calibration, water phantom measurements for PDD and beam profile or film measurements to evaluate the coincidence of light and radiation field size. Additionally, 3D γ analysis option in the software makes it more advantageous than 2D-based techniques. In this way, dose differences can be evaluated slice by slice on CT data and dose profile of the irradiated beam can also be analyzed in desired depth. However, novel system has some limitations that have to be pointed out. The first one is that the reconstruction model used in iViewDose is commissioned in homogenous conditions and inhomogeneity correction is not applied during the reconstruction of the dose distribution. Therefore, the accuracy of dose reconstruction is not adequate in the presence of large inhomogeneities such as lung. The second limitation is that electron contamination is not accounted in the reconstructed model and it can cause an uncertainty in the build-up region. This limitation needs to be taken into account during comparison of calculated and measured PDD values. Finally, iViewDose software does not have a correction for the effect of ghosting and it can cause an increase in the EPID pixel signal due to the exposure of the previous treatment field. Therefore, to reduce the uncertainties due to the ghosting effect, time interval between two subsequent measurements should be set as more than one minute.

Conclusion

iViewDose software working in conjunction with EPID iViewGT MV Panel was found as capable to perform basic machine-specific QC tests including daily output constancy, PDD and beam profile, coincidence of light and radiation fields size in a single irradiation of the reference treatment field during the morning checkout of the treatment machine. In addition to machine-specific QC test, novel in vivo dosimetry system provides a safety net for patient treatment by detecting major errors.

Compliance with ethical standards

Conflict of interest There is no conflict of interest.

Ethical approval This article does not contain any studies with human participants or animals performed by any of the authors.

References

1. McDermott LN, Louwe RJW, Sonke JJ, Van Herk M, Mijnheer BJ (2004) Dose–response and ghosting effects of an amorphous silicon electronic portal imaging device. Med Phys 31(2):285–295
2. Curtin-Savard AJ, Podgorsak EB (1999) Verification of segmented beam delivery using a commercial electronic portal imaging device. Med Phys 26:737–742
3. Pasma KL, Dirkx ML, Kroonwijk M, Visser AG, Heijmen BJ (1999) Dosimetric verification of intensity modulated beams produced with dynamic multileaf collimation using an electronic portal imaging device. Med Phys 26:2373–2378
4. Mans A, Remeijer P, Olaciregui-Ruiz I, Wendling M, Sonke J-J, Mijnheer B et al (2010) 3D Dosimetric verification of volumetric-modulated arc therapy by portal dosimetry. Radiother Oncol 94:181–187
5. van Elmpt W, McDermott L, Nijsten S, Wendling M, Lambin P, Mijnheer B (2008) A literature review of electronic portal imaging for radiotherapy dosimetry. Radiother Oncol 88:289–309
6. Esposito M, Bruschi A, Bastiani P, Ghirelli A, Pini S, Russo S, Zatelli G (2018) Characterization of EPID software for VMAT transit dosimetry. Austral Phys Eng Sci Med 41(4):1021–1027
7. Nijsten SM, Mijnheer BJ, Dekker AL, Lambin P, Minken AW (2007) Routine individualised patient dosimetry using electronic portal imaging devices. Radiother Oncol 83(1):65–75
8. Wendling M, Louwe RJW, McDermott LN, Sonke JJ, van Herk M, Mijnheer BJ (2006) Accurate two-dimensional IMRT verification using a back-projection EPID dosimetry method. Med Phys 33:259–273
9. Wendling M, McDermott LN, Mans A, Sonke JJ, van Herk M, Mijnheer BJ (2009) A simple backprojection algorithm for 3D in vivo EPID dosimetry of IMRT treatments. Med Phys 36:3310–3321
10. McDermott LN, Wendling M, Sonke JJ, van Herk M, Mijnheer BJ (2007) Replacing pretreatment verification with in vivo EPID dosimetry for prostate IMRT. Int J Radiat Oncol Biol Phys 67:1568–1577
11. Olaciregui-Ruiz I, Rozendaal R, Mijnheer B, Van Herk M, Mans A (2013) Automatic in vivo portal dosimetry of all treatments. Phys Med Biol 58(22):8253
12. Wendling M, McDermott NL, Mans A, Olaciregui-Ruiz I, Pecharromán-Gallego R, Sonke JJ et al (2012) In aqua vivo EPID dosimetry. Med Phys 39(1):367–377
13. Agarwal A, Rastogi N, Das KM, Yoganathan SA, Udayakumar D, Kumar S (2017) Investigating the electronic portal imaging device for small radiation field measurements. J Med Phys 42(2):59
14. Sun B, Goddu SM, Yaddanapudi S, Noel C, Li H, Cai B et al (2015) Daily QA of linear accelerators using only EPID and OBI. Med Phys 42(10):5584–5594

15. Budgell GJ, Zhang R, Mackay RI (2007) Daily monitoring of linear accelerator beam parameters using an amorphous silicon EPID. Phys Med Biol 52(6):1721
16. Dawoud SM, Weston SJ, Bond I, Ward GC, Rixham PA, Mason J et al (2014) Measuring linac photon beam energy through EPID image analysis of physically wedged fields. Med Phys 41(2):021708
17. van Elmpt WJ, Nijsten SM, Schiffeleers RF, Dekker AL, Mijnheer BJ, Lambin P et al (2006) A Monte Carlo based three-dimensional dose reconstruction method derived from portal dose images. Med Phys 33(7):2426–2434
18. Hægeland C. Optimization and verification of dosimetric robustness of VMAT dose-plans. Master of Science thesis. Norwegian University, 2016.